FAST INTERACTIVE MULTI-REGION CARDIAC SEGMENTATION WITH LINEARLY ORDERED LABELS

M. Rajchl[⋆†]*, J. Yuan*[⋆]*, E. Ukwatta*[⋆†] *and T.M. Peters*[⋆†]

[⋆] Robarts Research Institute Imaging Laboratories, London ON
[†] Biomedical Engineering Graduate Program, The University of Western Ontario, London ON

ABSTRACT

We present a novel and fast interactive approach to multi-modality cardiac image segmentation, which employs the linearly ordered surfaces as an additional constraint. We show using such a geometrical constraint helps to significantly reduce user interaction and improve the accuracy of segmentation results at the same time. We solve the proposed multi-region segmentation problem with the order constraints by means of convex optimization, resulting in a fast and reliable flow maximization approach which implicitly embeds the linear order prior without introducing extra computation load. In this regard, a new fully parallelized continuous max-flow algorithm is proposed and implemented using GPGPU to segment a 3D volume within one second. We demonstrate our results over pathological trans-esophageal echocardiogram, cardiac CT and delayed enhancement MRI data sets.

Index Terms— Image Segmentation, Max-Flow, MRI, Ultrasound, CT

1. INTRODUCTION

Finding multiple anatomical structures accurately and efficiently is a common task in medical image processing. In cardiac image processing, in particular extracted surfaces can be used as initialization for surface-based registration, measurements of ejection fraction (EF), left ventricular end-systolic volumes (LVESV), feature extraction and visualization, see [1] for reference. Segmenting such regions manually, or with intensive user input, is often time-consuming, subjective, sensitive to initialization and lacks repeatability [2, 3]. On the other hand, it is also challenging for fully automated methods to deliver clinically acceptable results due to the complexity of image features. In this regard, an apropriate degree of user guidance, i.e. interaction, along with prior information on the target objects, e.g. shape and region priors [4, 5] etc, will largely improve both efficiency and accuracy of most computer-based segmentation methods. In particular, some generic shape and region information, e.g. star-shape [6] or region orders [7], may help to significantly lower user input, while requiring only a slight increase in computational load or not. This is also in contrast to the cardiac segmentation method with strong spatial shape priors [8, 9, 10, 11] where extra learning and optimization steps are required, hence lead to a significant increase of computation and memory load.

In this work, we study a geometrical constraint of linearly nested surfaces within 3D volumes (for example, the thoracial cavity contains the heart, which further contains the blood volume), as a-priori knowledge to assist the segmentation of images volumes, independant of modality. Our experimental results demonstrate that, while it is intuitively simple, this approach is sufficiently powerful to produce clinically accurate and meaningful segments and the order prior is naturally embedded in the optimization procedure without additional computation cost. In practice, such nested surfaces can be properly represented by a sequence of regions containing each other. This type of constraint was first investigated by Ishikawa [12] over a specially designed graph, and recently re-studied and solved in the spatially continuous setting by [13, 14, 15] through convex optimization. Comparing to graph cut-based methods, the convex optimization-based approach works in the spatially continuous configuration and can neatly avoid grid bias which often appears as a visible side product from graph cut procedures, hence increase the segmentation accuracy. Moreover, the resulting algorithm can be implemented and parallelized on modern computing platforms, e.g. CUDA (NVIDIA Corp., Santa Clara, CA.), and make the optimization solver significantly faster than graph-cuts in practice, e.g. [16].

1.1. Contributions

In this paper, we introduce three volume labels (blood, myocardium and background), which represent the three regions overlapping each other in the order of the physical appearance of anatomical structures, and apply this order as geometrical constraint to assist the proposed 3D cardiac image segmentation. We build up the data cost functions based on a maximum log-likelihood of intensities by sampled histograms [17]. We propose a new fully parallelized continuous max-flow algorithm to the proposed variational multi-region volume segmentation problem, which results in a fast and reliable numerical solver on GPU. Without particularly optimizing its implementation, the proposed algorithm can obtain the clini-

cally acceptable accuracy of 3D cardiac segmentation within a second. In experiments, we test the sensitivity of the proposed approach to user initialization on cardiac image data sets of three different modalities and report a measure of overlap in form of a dice coefficient against a manually created gold standard as well as an average root means squared error of the resulting surfaces vertices. We also demonstrate its robustness towards initialization by letting non-expert users sample regions on random volume slices.

2. METHODS

The anatomical structures naturally introduce the prior information on the 3D cardiac image segmentation, where blood, myocardium and background are overlapped with each other. To enforce such a constraint definitely helps to improve the segmentation results. Moreover, we will show such a constraint can be well embedded in the proposed continuous max-flow optimization steps without increasing computation and memory load.

2.1. Segmentation with Ordered Labels

For the proposed algorithm, let Ω_i, $i = 1 \dots n-1$, denote the $n-1$ regions with a linearly overlapped order, such that

$$\Omega_n(=\emptyset) \subseteq \Omega_{n-1} \subseteq \ldots \subseteq \Omega_1 \subseteq \Omega_0(:=\Omega)\,. \quad (1)$$

Therefore, each segment $S_i := \Omega_{i-1} \backslash \Omega_i$, $i = 1 \dots n$, is just the area/volume between the two sequential surfaces. Given the image models ℓ_i, $i = 1 \dots n$, let $D_i(x)$ be the data fidelity function for each segment S_i which measures how well the local area around x fits the model ℓ_i. Then we can maximize the log-likelihood of our acquired normalized sample histogram according to Boykov and Jolly [17]:

$$D_i(x) = -\log P(I(x)|l_i) \quad (2)$$

We formulate the segmentation task as the following minimization problem:

$$\min_{S_i} \sum_{i=1}^{n} \int_{S_i} D_i(x)\, dx + \sum_{i=1}^{n-1} \alpha_i \int_{\partial\Omega_i} ds \quad (3)$$

subject to (1), where the second term penalizes the total perimeter of the $n-1$ nesting regions and encourages the segmentation with tight boundaries.

If we define the labeling functions $u_i(x) \in \{0,1\}$ such that

$$u_i(x) = \begin{cases} 1 & \text{if } x \in \Omega_i \\ 0 & \text{if } x \notin \Omega_i \end{cases}, \quad i = 1 \dots n-1\,.,$$

then the constraint of the $n-1$ linearly overlapped regions (1) just amounts to the following inequalities to the binary labeling functions $u_i(x)$:

$$0 \leq u_{n-1}(x) \leq \ldots \leq u_1(x) \leq 1\,, \quad \forall x \in \Omega\,. \quad (4)$$

We additionally define the functions $u_0(x) \equiv 1$ and $u_n(x) \equiv 0$, which just represent Ω and $\emptyset$ respectively.

With the aid of the labeling functions $u_i(x)$, $i = 0 \dots n$, the image segmentation problem (3) can be mathematically expressed as follows:

$$\min_{u_i \in \{0,1\}} \sum_{i=1}^{n} \int_{\Omega} (u_{i-1} - u_i) D_i\, dx + \sum_{i=1}^{n-1} \alpha_i \int_{\Omega} |\nabla u_i|\, dx \quad (5)$$

subject to the linear inequalities (4) of label orders, where the length term in (3) is properly encoded by the total-variation function.

2.2. Convex Relaxation and Continuous Max-Flow

Bae et al [15] proved that the non-convex optimization problem (5) can be solved globally and exactly through its convex relaxation model, i.e. the so-called *continuous min-cut model*:

$$\min_{u_i \in [0,1]} \sum_{i=1}^{n} \int_{\Omega} (u_{i-1} - u_i) D_i\, dx + \sum_{i=1}^{n-1} \alpha_i \int_{\Omega} |\nabla u_i|\, dx \quad (6)$$

subject to the linear inequalities (4), where the binary constraints $u_i(x) \in \{0,1\}$ are substituted instead of its convex relaxation $u_i(x) \in [0,1]$. The mathematical results are similar to those reported by Nikolova et al [18].

In addition, the authors proposed a *continuous max-flow model*:

$$\max_{p_i, q_i} \int_{\Omega} p_1\, dx \quad (7)$$

$$\text{s.t. } |q_i(x)| \leq \alpha_i\,,\ p_i(x) \leq D_i(x)\,, \quad (8)$$

$$\big(q_i - p_i + p_{i+1}\big)(x) = 0\,,\ i = 1 \dots n-1\,. \quad (9)$$

Its duality or equivalence to (6) was also constructed, where the labeling functions $u_i(x)$, $i = 1 \dots n-1$, are just the multiplier functions to the flow-preservation conditions (9) under the primal-dual perspective, i.e.

$$\max_{p_i, q_i} \min_{u_i \in [0,1]} L(p,q,u)\,, \quad \text{s.t. (8)}$$

where $L(p,q,u) := \int_{\Omega} p_1\, dx + \sum_{i=1}^{n-1} \langle u_i, q_i - p_i + p_{i+1} \rangle$.

The proposed flow-maximization framework (7) directly results in a fast numerical solver based on the modern convex optimization theory [19]. This is a similar approach as graph-cuts, where the fast solvers to the min-cut problems are often based on their dual max-flow models.

2.3. Fully Parallelized Continuous Max-Flow Algorithm

In this work, we adopt the convex min-cut/max-flow theory proposed in [15] to our specified segmentation problem along with the enforced label ordering prior (1), and observe that such problem can be solved globally and exactly. Moreover,

we propose a new continuous max-flow algorithm that can be fully parallelized and resulting in a more efficient solver on GPU. To see this, we follow the multiplier augmented method and define

$$L_c(p,q,u) \;=\; L(p,q,u) - \frac{c}{2}\sum_{i=1}^{n-1}\|q_i - p_i + p_{i+1}\|^2\,,$$

where $c > 0$ is constant.

The new continuous max-flow algorithm can therefore be summarized as follows: for the k-th iteration,

- Update all flow functions simultaneously, i.e.

$$q_i^{k+1}(x) \;:=\; \arg\max_{|q_i(x)|\le\alpha_i} L_c(p^k, q_i, q_{j\neq i}^k, u^k) \qquad (10)$$

$$p_i^{k+1}(x) \;:=\; \arg\max_{p_i(x)\le D_i(x)} L_c(p_i, p_{j\neq i}^k, q^k, u^k)\,; \quad (11)$$

- Update the labeling functions $u_i(x)$, $i = 1\ldots n-1$, by

$$u_i^{k+1}(x) \;=\; u_i^k(x) - c\big(q_i - p_i + p_{i+1}\big)(x)\,.$$

The steps (10) and (11) of the above algorithm are distinct from Bae's continuous max-flow algorithms [15] which explore the optimization of the dual flow functions over each layer sequentially. In practice, the new parallelized scheme enjoys a faster convergence.

3. EXPERIMENTS

We implemented the aforementioned algorithm with a graphical user interface and parallelized it using CUDA to achieve both maximum interactivity and a high computational efficiency, e.g. it segments the 3D cardiac volume with three regions in one second. To cope with widespread image intensity ranges (i.e. CT Houndsfield units), we employed 32 bin histograms for the maximum likelihood calculations of each sample. The user was provided with three plane views and a 3D scene containing the resulting segmentation labels as rendered surfaces. The user can brush over the plane views to sample intensities belonging to each label to feed the histograms for maximum likelihood calculation. Additionally we added a 2D region-growing algorithm for optional faster sampling from these views. The two total variation regularization weights α_1 and α_2 from equation (6) are accessible from the interface. Resulting continuous segmentation labels from the optimization procedure were thresholded by a value of 0.5 to discretize them and obtaining binary labels. After a short introduction on how to use the interface, three non-expert users were asked segment blood volume, myocardial/vascular tissue and background respectively and repeat this process five times with sampling on random inital slices. Three image volumes from three different imaging modalities were emplyed in our study: 3D trans-esophageal echocardiograms (TEE) (Philips Healthcare, Andover, MA), contrast-enhanced inversion recovery MRIs (Siemens Medical Solutions, Malvern, PA) and cardiac CT (GE Healthcare, Pewaukee, WI). These images were cropped to a maximum region of interest containing the entire visible heart. The gold standard against which the output of our algorithm was compared were manual segmentations of the target structures. A dice coefficient was employed as a measure of similarity. It was weighted against the respective label size and the overlap of all labels added to reflect the combined similarity of all segmentation labels in each volume.

3.1. Results

Figure 3.1 shows surface-rendered results from three of our segmentations. To visualize all three labels, the respective opacities were set to 33% for background/thorax cavity, 66% for myocardial/vascular tissue and 100% for the blood volume. From left to right we rendered one trans-esophageal echocardiogram, a constrast-enhanced MRI and a cardiac CT.

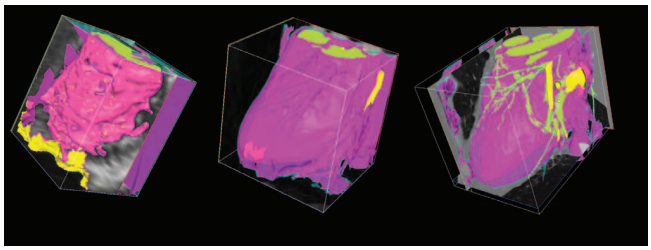
The resulting dice metric (DM) and root mean squared error (RMSE) for blood volume(b) and myocardial tissue (m) in [mm] is reported in Tab 1. The RMSE represents the average error for the vertices of all surfaces. Resulting dice coefficients from our segmentations have a fairly low standard deviation suggesting robustness towards user input, while resulting in acceptably high accuracies. Further, we observe that vascular trees are clearly visible and accurately containing the blood volume surface within the vascular/myocardial surface.

DataSet	DM $\{0,1\}$	RMSE(b)	RMSE(m)
CT - 1	0.88 ± 0.02	0.61 ± 0.93	0.80 ± 0.92
CT - 2	0.88 ± 0.02	0.94 ± 1.56	0.71 ± 1.09
CT - 3	0.87 ± 0.07	0.80 ± 1.27	0.86 ± 1.38
mean	$\mathbf{0.88 \pm 0.04}$	$\mathbf{0.78 \pm 1.25}$	$\mathbf{0.79 \pm 1.13}$
ceMRI - 1	0.93 ± 0.02	0.51 ± 0.85	0.33 ± 0.58
ceMRI - 2	0.84 ± 0.03	0.76 ± 1.02	1.70 ± 2.32
ceMRI - 3	0.91 ± 0.03	0.48 ± 0.90	0.47 ± 0.84
mean	$\mathbf{0.90 \pm 0.03}$	$\mathbf{0.58 \pm 0.93}$	$\mathbf{0.83 \pm 1.25}$
TEE - 1	0.81 ± 0.03	0.64 ± 0.71	1.11 ± 1.34
TEE - 2	0.90 ± 0.01	0.22 ± 0.29	0.19 ± 0.52
TEE - 3	0.86 ± 0.02	0.30 ± 0.34	0.30 ± 0.32
mean	$\mathbf{0.86 \pm 0.02}$	$\mathbf{0.39 \pm 0.45}$	$\mathbf{0.53 \pm 0.73}$

Table 1. Segmentation results from cardiac CT

4. CONCLUSIONS

We demonstrate a novel interactive approach to multi-modality 3D cardiac image segmentation, which applies the order of



Surface-rendered segmentation results

nested regions as the additional constraint. Experiments show such a constraint helps to both lower user interaction and improve the accuracy of segmentation results. The new fully-parallelized continuous max-flow algorithm is proposed and implemented on GPU to achieve a high efficiency of 3D multi-region cardiac segmentation. We also test the reliability and robustness of the proposed approach over MRI, cardiac CT and TEE image data sets.

The proposed continuous max-flow approach is fairly general, which makes it feasible to other medical segmentation tasks with a linearly overlapped order of regions, such as brain and abdominal organ segmentation. Moreover, other generic shape priors, e.g. star-shape etc, can be added to this Max-Flow framework to improve segmentation accuracy and efficiency.

5. REFERENCES

[1] Wolfgang Birkfellner, *Applied Medical Image Processing: A Basic Course*, CRC Press, 2011.

[2] Paul A. Yushkevich, Joseph Piven, Heather Cody Hazlett, Rachel Gimpel Smith, Sean Ho, James C. Gee, and Guido Gerig, "User-guided 3D active contour segmentation of anatomical structures: Significantly improved efficiency and reliability," *Neuroimage*, vol. 31, no. 3, pp. 1116–1128, 2006.

[3] Andrew Top, Ghassan Hamarneh, and Rafeef Abugharbieh, "Active learning for interactive 3d image segmentation," in *Medical Image Computing and Computer-Assisted Intervention (MICCAI)*. 2011, vol. 6893 of *LNCS*, pp. 603–610, Springer Berlin / Heidelberg.

[4] Andrew Delong and Yuri Boykov, "Globally optimal segmentation of multi-region objects.," in *ICCV'09*, 2009, pp. 285–292.

[5] Qi Song, Xiaodong Wu, Yunlong Liu, M. Sonka, and M. Garvin, "Simultaneous searching of globally optimal interacting surfaces with shape priors," in *CVPR 2010*, june 2010, pp. 2879 –2886.

[6] Olga Veksler, "Star shape prior for graph-cut image segmentation," in *ECCV*, 2008, pp. 454–467.

[7] Pedro F. Felzenszwalb and Olga Veksler, "Tiered scene labeling with dynamic programming," in *CVPR*, 2010, pp. 3097–3104.

[8] Nikos Paragios, "A level set approach for shape-driven segmentation and tracking of the left ventricle," *IEEE Trans. Med. Imaging*, vol. 22, no. 6, pp. 773–776, 2003.

[9] Honghai Zhang, Andreas Wahle, Ryan K. Johnson, Thomas D. Scholz, and Milan Sonka, "4-d cardiac mr image analysis: Left and right ventricular morphology and function," *IEEE Trans. Med. Imaging*, vol. 29, no. 2, pp. 350–364, 2010.

[10] Mohammad Saleh Nambakhsh, Jing Yuan, Ismail Ben Ayed, Kumaradevan Punithakumar, Aashish Goela, Ali Islam, Terry M. Peters, and Shuo Li, "A convex max-flow segmentation of lv using subject-specific distributions on cardiac mri," in *IPMI*, 2011, pp. 171–183.

[11] Ismail Ben Ayed, Kumaradevan Punithakumar, Shuo Li, Ali Islam, and Jaron Chong, "Left ventricle segmentation via graph cut distribution matching," in *MICCAI (1)*, 2009, pp. 901–909.

[12] H. Ishikawa, "Exact optimization for markov random fields with convex priors," *IEEE Transactions on Pattern Analysis and Machine Intelligence*, vol. 25, pp. 1333–1336, October 2003.

[13] A. Chambolle, D. Cremers, and T. Pock, "A convex approach for computing minimal partitions," Tech. Rep. TR-2008-05, University of Bonn, November 2008.

[14] J. Yuan, E. Bae, and X.C. Tai, "A study on continuous max-flow and min-cut approaches," in *CVPR*, USA, San Francisco, 2010.

[15] E. Bae, J. Yuan, X.-C. Tai, and Y. Boycov, "A study on continuous max-flow and min-cut approaches part ii: Multiple linearly ordered labels," Technical report CAM-10-62, UCLA, 2010.

[16] M. Rajchl, J. Yuan, and T.M. Peters, "Real-time segmentation in 4d ultrasound with continuous max-flow," in *SPIE Medical Imaging*, USA, San Diego, 2012.

[17] Y. Boykov and M.P. Jolly, ," in *Interactive Graph Cuts for Optimal Boundary & Region Segmentation of Objects in N-D Images*. International Conference on Computer Vision (ICCV), 2001, vol. I, pp. 105–111.

[18] Mila Nikolova, Selim Esedoglu, and Tony F. Chan, "Algorithms for finding global minimizers of image segmentation and denoising models," *SIAM J. App. Math.*, vol. 66, no. 5, pp. 1632–1648, 2006.

[19] Dimitri P. Bertsekas, *Nonlinear Programming*, Athena Scientific, September 1999.